J. Chem. Sci. (2022)134:53
https://doi.org/10.1007/s12039-022-02027-3

REGULAR ARTICLE

2-Mercaptobenzimidazole ligand-based models of the [FeFe] hydrogenase: synthesis, characterization and electrochemical studies

NAVEEN KUMAR and SANDEEP KAUR-GHUMAAN*
Department of Chemistry, University of Delhi, Delhi 110007, India
E-mail: skaur@chemistry.du.ac.in

MS received 15 September 2021; revised 11 December 2021; accepted 13 December 2021

Abstract. Reaction of $Fe_3(CO)_{12}$ and 2-mercaptobenzimidazole leads to the formation of a triiron sulphur cluster $[Fe_3(C_7H_6N_2)(\mu_3\text{-}S)_2(CO)_8]$ **1** and a diiron monothiolate-bridged complex $[Fe_2(\mu\text{-}2\text{-mercaptobenzimidazole})_2(CO)_6]$ **2**. The structures of the complexes were confirmed by various spectroscopic techniques (NMR, FTIR, UV-Vis), elemental analysis and mass spectrometry. FTIR spectra of **1** and **2** (in CH_2Cl_2) displayed peaks at 2069, 2022, 2006, 1965 and 2070, 2002, 1963 cm^{-1}, respectively indicating the presence of terminal carbonyls in the two complexes. Based on cyclic voltammetric measurements, complexes **1** and **2** were found to catalyze the reduction of trifluoroacetic acid to produce dihydrogen (in CH_3CN) at −1.68 V and −1.58 V *vs.* Fc/Fc^+, respectively.

Keywords. Dinuclear; Electrocatalysis; [FeFe] Hydrogenases; Hydrogen; N-based ligands; Trinuclear.

1. Introduction

The $[Fe_2S_2]$ core with a bridging thiolato ligand known to be a part of the [FeFe] hydrogenase enzyme active site (also known as the H-cluster) has been of great interest to researchers over several decades. This is because the iron-only enzyme is known to catalyze the reversible interconversion of protons to dihydrogen with high turnovers at neutral pH.[1,2] With an aim to develop inexpensive and efficient catalysts for the generation of hydrogen, a large number of organometallic models of the H-cluster have been studied.[3–9] The models have been designed using different combinations of bridging (thiolato) and terminal (CO, CN^-, phosphines and carbenes) ligands.[3–9] Though attempts to model the exact structure of the active site have been successful to some extent, the performance of the mimics has been limited by high overpotential, low turnover, and stability of the hydride intermediates, reduction of protons at highly negative potentials and their stability.[3–10]

In an attempt to shift the reduction potential of the complexes to less negative values, either electron-withdrawing groups or N-containing moieties have been introduced as part of the aromatic thiolate bridge.[6e,8d,11–15] The electron-density at the metal center and hence, the reduction potential of the complexes can be lowered due to the presence of electron-withdrawing or N-containing groups in the thiolate framework. Though a few all carbonyl models of N-containing dithiolate bridges are known: $[Fe_2(\mu$-quinoxaline-2,3-dithiolate$)(CO)_6]$, $[Fe_2(\mu$-pyrido[2,3b]pyrazine-2,3-dithiolate$)(CO)_6]$, $[Fe_2(\mu$-diph-6,7-qdt$)(CO)_6]$, $[Fe_2(\mu$-btdt$)(CO)_6]$, $[Fe_2(\mu$-pyrazine-2,3-dithiolate$)(CO)_6]$, $[Fe_2\{2\text{-}\mu\text{-}SC_5H_3N\text{-}3\text{-}(CO)S\text{-}\mu\}(CO)_6]$, $[Fe_2(\mu$-naphthalenemonoimide dithiolate$)(CO)_6]$, $[Fe_2(mcbdt)(CO)_6]$, $[Fe_2\{\mu$-qdt$\}(CO)_6]$ and $[Fe_2\{\mu$-ppdt$\}(CO)_6]$,[3c,6e] there are only few examples of such type of monothiolate ligand-based iron carbonyl (structural or functional) complexes (**a**–**j**) (Figure 1).[8b,9,15c,16]

Further, even though tremendous number of diiron systems have been reported as electrocatalysts for proton reduction to dihydrogen,[3–9] there are only a few examples of triiron cluster complexes (**k**–**r**) (Figure 2) that have been explored so far.[17–24] Cluster complexes with more than two metal centers have been of particular interest since they can act as electron reservoirs and also involve in multi-electron redox

*For correspondence
Supplementary Information: The online version contains supplementary material available at https://doi.org/10.1007/s12039-022-02027-3.

Published online: 08 April 2022

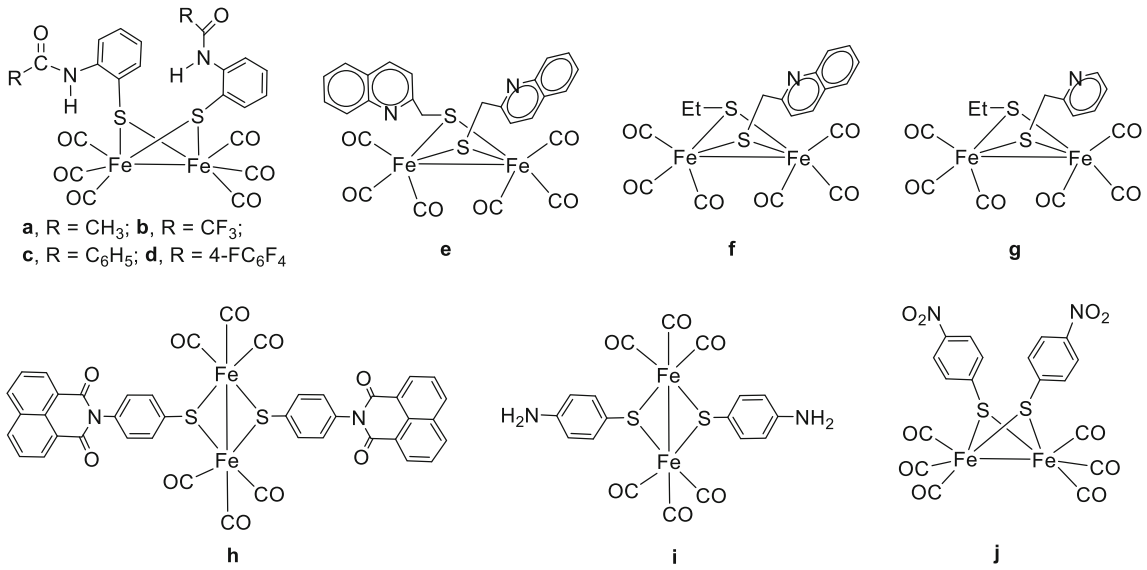

Figure 1. Reported structural and functional complexes with aromatic N-containing bis(monothiolato) linkers.[8b,9,15c,16]

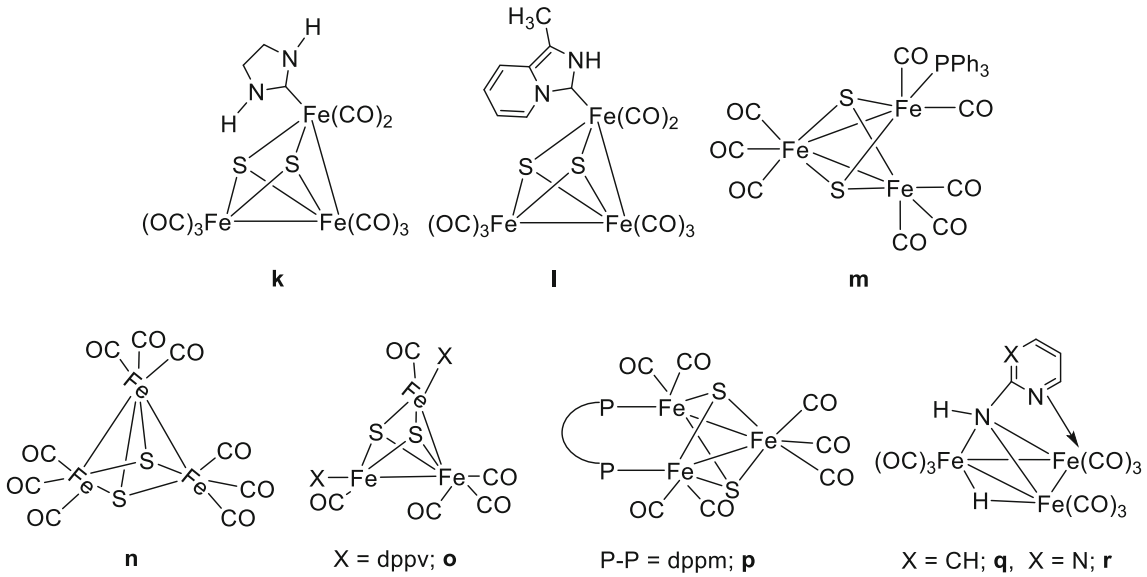

Figure 2. Representative structural and functional triiron cluster complexes.[18–24]

processes.[21–27] In an attempt to manipulate the reduction potential of the complexes, ligands with electron-donating/withdrawing groups containing P-, N- or S-donor sites have been introduced.[3–10] In this context, nucleophilic N-heterocyclic carbene ligands (NHC) are an important class of ligands that have been incorporated into organometallic electrocatalytic systems as these ligands are bulkier and more basic than the ubiquitous phosphines.[28,29]

Based on the above-mentioned facts and that bioinspired hydrogenase multinuclear carbonyl models with more than two iron centers have received much less attention, in this work synthesis, spectroscopic and electrochemical characterization of a triiron sulphur cluster complex $[Fe_3(C_7H_6N_2)(\mu_3\text{-}S)_2(CO)_8]$ **1** containing a carbene unit attached to one of the iron centers and a bis(monothiolato) diiron complex $[Fe_2(CO)_6(\mu\text{-}2\text{-mercaptobenzimidazole})_2]$ **2** are presented. Complex **1** was isolated as a by-product from the reaction of $Fe_3(CO)_{12}$ with the monothiolate ligand 2-mercaptobenzimidazole while synthesizing the target complex **2**. In contrast, unusual N-heterocyclic carbene complexes **k** and **l** (Figure 2) have been obtained by the reaction of $Fe_3(CO)_{12}$ with $(CH_2\text{-}NH)_2CS$ in refluxing tetrahydrofuran (THF) and $[HNEt_3][2\text{-}C_5H_4NCH(CH_3)NHCS_2]$ with PhCOCl at

room temperature, respectively.[18] The diiron thiolate-bridged carbene complexes on the other hand, have been mostly synthesized by the reactions of the all-carbonyl iron complexes [Fe_2(μ-S-X-S-μ)$(CO)_6$] with *in situ* generated carbene ligands.[28,29]

Furthermore, the electrocatalytic reduction of acetic acid (weak acid) and trifluoroacetic acid (moderately strong acid) in CH_3CN by complexes **1** and **2** have been discussed in this work. Complex **1** however, failed to show electrocatalysis with acetic acid. A comparison of the electrochemical properties of complex **1** with other reported triiron clusters (**n–r**),[21–24] diiron NHC-based models and of complex **2** with similar models incorporating N-based linkers (di- or monothiolates) have been delineated.[28,29]

2. Experimental

2.1 *Materials and physical measurements*

The syntheses of the complexes were conducted under argon (Ar) atmosphere using standard Schlenk line techniques. Triirondodecarbonyl ($Fe_3(CO)_{12}$), 2-mercaptobenzimidazole and solvents $CDCl_3$, anhydrous tetrahydrofuran (THF), anhydrous acetonitrile (CH_3CN) were purchased from Sigma-Aldrich and used without further purification.

Elemental analysis was performed on the Elementar Alysensysteme GmbH Vario EL Cube Elemental analyser. Infra-red spectra were recorded in dichloromethane over the range 400–4000 cm^{-1} on Bruker Alpha (ZnSe) FTIR Spectrometer. ^1H NMR spectra were recorded at room temperature in $CDCl_3$ on a JEOL JNM-EXCP 400 MHz spectrometer. Mass spectra were recorded with Bruker Maxis Impact (282001.00081) mass spectrometer and (Agilent G6530AA (LC-HRMS-Q-TOF) Quadrupole Time-of-flight mass spectrometer with ESI and APCI sources. The UV-Vis spectra for the complex were recorded on Analytik Jena Specord 250 UV-Vis spectrophotometer.

Cyclic voltammograms (CVs) were measured in acetonitrile using a Metrohm Autolab Potentiostat (PGSTAT302N) with a GPES electrochemical interface (EcoChemie). All CVs were measured under argon at a scan rate of 0.1 Vs^{-1}, unless otherwise mentioned. Tetrabutylammonium hexafluorophosphate dried in vacuum at 383 K (0.1 M) (Sigma-Aldrich, electrochemical grade) was used as the supporting electrolyte. The working electrode was a glassy carbon disc (diameter 3 mm, freshly polished). Platinum wire was used as the counter electrode. The reference electrode was a non-aqueous Ag/Ag^+ electrode (CH Instruments, 0.01 M $AgNO_3$ in acetonitrile). All potentials are quoted against the ferrocene-ferrocenium couple (Fc/Fc^+) and the solutions were prepared from anhydrous acetonitrile (dried with molecular sieves (MS) 3Å). Controlled potential coulometry (CPC) was performed with the same instrument and three-electrode set-up described earlier. The experiment was carried out with continuous stirring and purging of argon gas at a fixed potential.

2.2 *Synthesis of complexes [$Fe_3(C_7H_6N_2)$-$(\mu_3$-$S)_2(CO)_8$] **1** and [$Fe_2(CO)_6$(μ-2-mercaptobenzimidazole)$_2$] **2***

A THF solution of triirondodecacarnonyl (0.250 g, 0.496 mmol) and 2-mercaptobenzimidazole (0.164 g, 1.09 mmol) was purged with argon and refluxed for 1.5 h. The colour of the solution changed from green to red-brown. After removal of the solvent by rotary evaporation, the mixture was subjected to purification on a silica gel column. Elution with n-pentane afforded a violet solution **n**. Elution with a mixture of hexane/dichloromethane (7:3 v/v) followed by elution with dichloromethane afforded red-brown and dark orange solutions for complexes **1** and **2**, respectively. These complexes were scratched as air-stable solids after removal of solvent.

Complex **1**: From the main red-brown band, ~ 0.120 g (42%) of **1** was obtained as a red-brown solid. FTIR (CH_2Cl_2, cm^{-1}): $\nu_{C=O}$ 2069(vs), 2022(m), 2006(m), 1965(s). FTIR (KBr disc, cm^{-1}): ν_{NH} 3445(m); $\nu_{C=O}$ 2067(s), 2029(vs), 1995(m,br). ^1H NMR (400MHz, $CDCl_3$): 9.60 (s, 2H, NH proton), 7.40–7.08 (m, 4H, aromatic protons) ppm. Anal. Calcd. for $C_{15}H_6Fe_3N_2O_8S_2$: C, 31.39; H, 1.05; N, 4.88; S, 11.17. Found: C, 32.11; H, 1.15; N, 4.86; S, 10.99%. LC-MS (ESI) (*m/z*): Calcd. 573.88. Found, 596.59 $[M+ Na]^+$. UV-vis (λ): 295, 352(CH_2Cl_2); 288, 353(CH_3CN); 301 (CH_3CN:H_2O) (7:3).

Complex **2**: From the main dark orange band, ~ 0.021 g (7%) of **2** was obtained as a dark orange solid. FTIR (CH_2Cl_2, cm^{-1}): $\nu_{C=O}$ 2070(s), 2002(m,br), 1963(m). FTIR (KBr disc, cm^{-1}): ν_{NH} 3451(m); $\nu_{C=O}$ 2070(s), 2028(vs), 1984(m,br). ^1H NMR (400 MHz, $CDCl_3$): 8.44 (s, 2H, NH), 8.02–8.48 (m, 8H, thiolate ligand) ppm. Anal. Calcd. for $C_{20}H_{10}Fe_2N_4O_6S_2$: C, 41.51; H, 1.73; N, 9.69; S, 11.07. Found: C, 41.88; H, 1.98; N, 9.80; S, 11.11%. LC-MS (ESI) (*m/z*): Calcd. 578.14. Found, 579.29 $[M+ H]^+$.

2.3 *X-ray crystallography*

Single crystals for complex **1** were grown by slow evaporation of hexane/dichloromethane (1:1) mixture at low temperature. X-ray data of the complex was collected on an Oxford Xcalibur CCD single-crystal X-ray diffractometer at 293 K, equipped with graphite monochromatic MoKα radiation (λ = 0.71073 Å). Significant crystallographic parameters and refinement details and selected bond distances and bond angles for complex **1** are listed in Tables S1 and S2, SI. The crystal structure of the complex was solved by direct methods using SIR-92[30a] and refined by full-matrix least-squares refinement techniques on F2 using SHELXL-97.[30b] The structure was solved and refined by standard procedures. The multi-scan absorption correction was applied. The coordinates of nonhydrogen atoms were refined anisotropically using SHELXL-J.[30c] All calculations were done using the Olex2 1.3 software. For the molecular graphics, the program ORTEP-3 was used.[31]

3. Results and Discussion

3.1 *Synthesis and characterization*

Air and moisture- stable triiron carbonyl cluster complex $[Fe_3(C_7H_6N_2)(\mu_3\text{-}S)_2(CO)_8]$ **1** and a dinuclear iron complex $[Fe_2(CO)_6(\mu\text{-}2\text{-mercaptobenzimidazole})_2]$ **2** were synthesized by refluxing 2.2 equivalents of 2-mercaptobenzimidazole with 1 equivalent of $Fe_3(CO)_{12}$ in THF under argon atmosphere for 1.5 h. (Scheme 1). A similar reaction in toluene or acetonitrile yielded only complex **1**. The reaction mixture was purified by column chromatography on silica gel using pentane and hexane/dichloromethane as eluting solvents. A violet-coloured triiron cluster **n** was obtained as a minor product on elution with pentane. Formation of **n** has also been reported earlier on reaction of monothiolate ligands with triirondodecarbonyl.[32] Red-brown and orange-coloured solids corresponding to complexes **1** and **2**, respectively were obtained after the removal of solvents. Complex **1** was isolated as a by-product during the synthesis of the target complex **2** which was obtained in very low yields. However, synthesis of complex **2** as the major product and its spectroscopic characterization have been reported earlier by Zheng and co-workers.[16b]

Single crystals for complex **1** were grown from a hexane/dichloromethane (1:1) mixture at low temperature. In the case of complex **2**, single crystals were not obtained despite several attempts. The molecular structure of **1** was confirmed by X-ray diffraction analysis. Since the structure for complex **1** is already reported by An and co-workers,[17] therefore, for the ORTEP diagram, crystallographic parameters, selected bond distances and angles see Figures S1, S2 and Tables S1, S2, SI. As seen from the ORTEP diagram, complex **1** is a trinuclear iron monocarbene complex with a distorted square-based pyramidal geometry, with two $Fe(CO)_3$ units and one $Fe(CO)_2$ (monocarbene) unit. The two-electron carbene group replaced one apical (axial) CO ligand.[18] The planarity of the N-heterocyclic carbene ligand (sp^2-hybridisation) was confirmed from the sum of the angles (359.6 $(3)^0$) around the C(1), i.e. N(1)-C(1)-Fe(1) (127.5$(3)^0$), N(1)-C(1)-N(2) (104.5$(3)^0$), N(2)-C(1)-Fe(1) (127.6$(3)^0$).[18] The other bond distances and angles matched with those of similar reported complexes (**k** and **l**).[18,33–36]

The complexes were characterized by elemental analysis, mass spectrometry and FTIR, UV-Vis and NMR spectroscopic techniques (Figures S3–S7, SI). FTIR spectra for complexes **1** and **2** were recorded in both solution (dichloromethane) and solid phase (KBr pellet) (Table 1 and Figure S3, SI). The KBr pellet FTIR spectra were broad while well-resolved spectra were displayed in the liquid phase.[37] FTIR data for complexes **1** and **2** and for analogous reported complexes are presented in Table 1. In the FTIR spectra (CH_2Cl_2), the carbonyl stretching frequencies for **1**

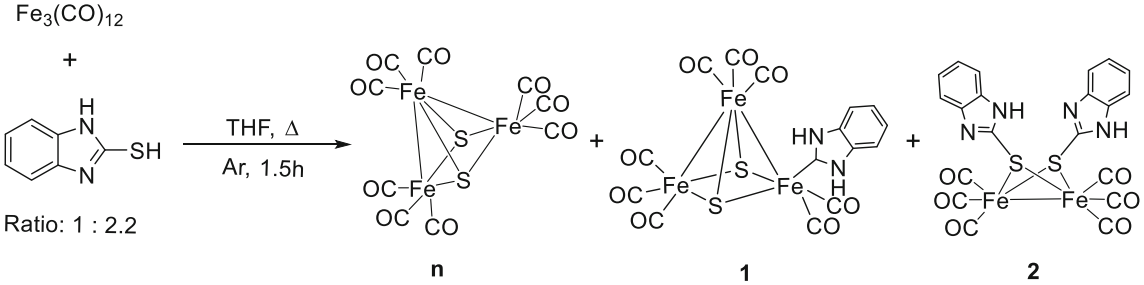

Scheme 1. Synthesis of complexes $[Fe_3(C_7H_6N_2)(\mu_3\text{-}S)_2(CO)_8]$ **1** and $[Fe_2(CO)_6(\mu\text{-}2\text{-mercaptobenzimidazole})_2]$ **2**.

Table 1. FTIR data for complexes **1** and **2** and other reported analogous complexes in dichloromethane.

Complex	Wavelength/cm^{-1}	Ref.
1	2069, 2022, 2006, 1965	This work
	2067, 2029, 1995[a]	This work
2	2070, 2002, 1963	This work
	2070, 2028, 1984[a]	This work
a	2074, 2037, 1998	15c
b	2077, 2042, 2003	15c
c	2075, 2038, 1999	15c
d	2076, 2040, 2001	15c
e	2072, 2038, 1997	16a
f	2072, 2037, 1998	16a
g	2072, 2036, 1995	16a
h	2075, 2040, 2000	9
i	2070, 2035, 1995	9
j	2080, 2044, 2003	8b
k	2068, 2009[a]	18
l	2069, 2037, 1998, 1994[a]	18
n	2063, 2044, 2024, 2006, 1985[b]	21
	2062, 2043, 2021	

[a]KBr, [b]n-hexane.

observed at 2069, 2022, 2006, 1965 and for **2** at 2070, 2006, 1963 cm^{-1} can be assigned to terminal metal carbonyls. The ν_{CO} values for **1** and **2** were in the same range as analogous triiron monocarbene (**k**, **l**)[18] (Table 1) and diiron monothiolate complexes, respectively.[8,16b]

The ^{1}H NMR spectrum of complex **1** displayed similar peaks as that reported in literature[17,18,36b] while the ^{1}H NMR spectrum for complex **2** showed multiplets at 8.02 and 8.48 ppm for the eight aromatic protons and a singlet at 8.44 pm for the two NH protons of the two monothiolate ligands (Figure S4, SI). The positive-ion ESI mass spectra of **1** and **2** displayed signals at a mass-to-charge ratio (m/z) 596.59 and 579.29 which correspond to $[\mathbf{1}+Na]^+$ and $[\mathbf{2}+H]^+$ (Figures S5 and S6, SI), respectively. Further, in the UV-Vis absorption spectra for complex **1** peaks were displayed at 295, 352; 289, 353 and 301 in CH_3CN, CH_2Cl_2, CH_3CN:H_2O (7:3), respectively (Figure S7 and Table S3, SI). No significant influence of solvent polarity was observed in the spectra measured in different solvents thus, suggesting a delocalized ground-state electronic structure.[23,38] The absorption bands can be assigned to d-d transitions (transitions within the σ-bonded Fe3 triangular core) (for **1**).[23] For complex **2** spectrum similar to previously reported complexes $[Fe_2(CO)_4(\mu\text{-naphthalene-2-thiolate})_2]$, $[Fe_2(\mu\text{-}SC_6H_4CH_3\text{-}p)_2(CO)_6]$ (340 nm) was displayed.[8] The UV-Vis spectra in CH_3CN/H_2O mixture did not show any major change, thus, suggesting that the complexes were possibly stable in aqueous media (Figure S7 and Table S3, SI).

3.2 *Electrochemistry*

Electrochemical investigations were performed for both complexes **1** and **2** in CH_3CN under argon atmosphere. Cyclic voltammograms (CVs, 0.1 Vs^{-1}) for complex **1** displayed one-electron irreversible reduction at E_{pc} = −1.51 V and an irreversible oxidation at E_{pa} = 0.51 V (Table 2 and Figure S8, SI). A small reduction peak was also observed at −1.07 V, similar to the values reported for other triiron clusters.[21–23] CVs for complex **2** displayed irreversible reductions peaks at −1.20 and −1.47 V and oxidation peak at 0.88 V (Table 2 and Figure S8, SI). The linearity of the Randles-Sevcik plot for the reduction and oxidation processes indicate diffusion-controlled processes without electrode deposition[39] (Figure S9, SI). The reversibility of the peak at −1.51 V did not improve much at higher scan rates. Further at longer time scales, more than one electron may be involved in the reduction process as evident by the slight deviation from linearity at scan rates below 0.05 Vs^{-1} (Figure S9, SI).[24] The reduction can be assigned as Fe^{I}-$Fe^{II}Fe^{I}\rightarrow Fe^{I}Fe^{I}Fe^{I}$ and the oxidation as $Fe^{I}Fe^{II}$ $Fe^{I}\rightarrow Fe^{II}Fe^{II}Fe^{I}$ redox processes.[22] The reductions for reported triiron cluster complexes $[Fe_3(\mu_3\text{-}S)_2(CO)_9]$ **n**, $[Fe_3(\mu_3\text{-}S)_2(CO)_7(dppm)]$ **p**, $[Fe_3(CO)_9(\mu_3\text{-pyNH})(\mu\text{-H})]$ **q** and $[Fe_3(CO)_9(\mu_3\text{-pymNH})(\mu\text{-H})]$ **r** have been shown to occur at −1.03, −1.75; −1.43, −1.61 and −1.47 V, respectively.[21,23,24] On the contrary, the reduction for complex **1** occurred at a more negative potential than complex **n** due to the presence of a basic carbene ligand on one of the iron centers (Table 2).

Complexes **1** and **2** were further investigated for electrocatalytic activity with acetic acid (AcOH) and trifluoroacetic acid (TFA) as proton sources. Complex **1** did not show any catalytic response with acetic acid (weak acid). However, with TFA the reduction peak at −1.51 V slowly disappeared (Figure 3a) on the addition of up to 19 mM of acid and two new reduction peaks were observed at −1.68 V and −2.00 V (19 mM) for complex **1** (Figure 3). The current for both the new reduction peaks increased and the peaks shifted cathodically on further addition of acid. The small reduction peak at −1.07 V shifted only anodically without any increase in current (1–10 mM) (Figure 3a). The catalytic currents levelled off after ∼ 250 mM of acid addition.

Table 2. Electrochemical data for aromatic N-containing bis(monothiolato) linkers and triiron cluster complexes in acetonitrile.

Complex	E_{pc}/V	Acid	$\left(\frac{i_{cat}}{i_p}\right)_{max}$	E_{cat}/V	*TOF*/ s^{-1}	O.P/ V	Ref.
$[Fe_3(C_7H_6N_2)(\mu_3\text{-}S)_2(CO)_8]$ **1**	−1.51	TFA	23.0	−1.68 −2.00	102	0.79	This work
$[Fe_2(\mu\text{-}2\text{-mercaptobenzimidazole})_2(CO)_6]$ **2**	−1.20	AcOH	–	−2.32	–	0.82	This work
	−1.47	TFA	40.3	−1.58 −1.85	315	0.67	This work
$[\{\mu\text{-}S\text{-}2\text{-}(4\text{-}FC_6H_4CONHC_6H_4)\}_2Fe_2(CO)_6]$ **d**	−1.19 −1.66	AcOH	1.48	−2.27	0.42	0.81	[15c]
$[Fe_2(\mu\text{-}N\text{-}(4\text{-thiolphenyl})\text{-}1,8\text{-naphthalimide})_2(CO)_6]$ **h**	−1.61 −1.74	AcOH	8.33	−2.19	13.4	0.73	[9]
$[Fe_2(\mu\text{-}4\text{-aminothiolphenol})_2(CO)_6]$ **i**	−1.53	AcOH	8.20	−1.88	13.0	0.42	[9]
$[Fe_2(\mu\text{-}SC_6H_4\text{-}p\text{-}NO_2)(CO)_6]$ **j**	−1.29	AcOH	12.0	∼ −2.2	27.8	0.74	[8b]
$[Fe_3(\mu_3\text{-}S)_2(CO)_9]$ **n**	−1.03[a, b] −1.75[a, b]	HBF_4 .Et_2O	2.13	−1.00 −1.30	0.88	0.72	[21a]
	−0.94 −1.75	AcOH	18.0	−2.24	62.7	0.78	[21b]
$[Fe_3\ (\mu_3\text{-}S)_2(CO)_5(dppv)_2]$ **o**	−2.05[b]	HOTf	13.0	−0.98	32.7	–	[22]
$[Fe_3\ (\mu_3\text{-}S)_2(CO)_7(dppm)]$ **p**	−1.43	TFA	2.91	−1.37	1.64	0.54	[23]
	−1.60 [b]		4.81	−1.48 [b]	4.50	–	[23]
$[Fe_3(CO)_9(\mu_3\text{-pyNH})(\mu\text{-H})]$ **q**	−1.61	*p*-TsOH	7.00	−1.77 −1.94	9.48	1.12	[24]
$[Fe_3(CO)_9(\mu_3\text{-pymNH})(\mu\text{-H})]$ **r**	−1.47	*p*-TsOH	7.50	−1.24 −1.69	10.9	0.59	[24]

[a] $E_{1/2}$ value. [b] In CH_2Cl_2

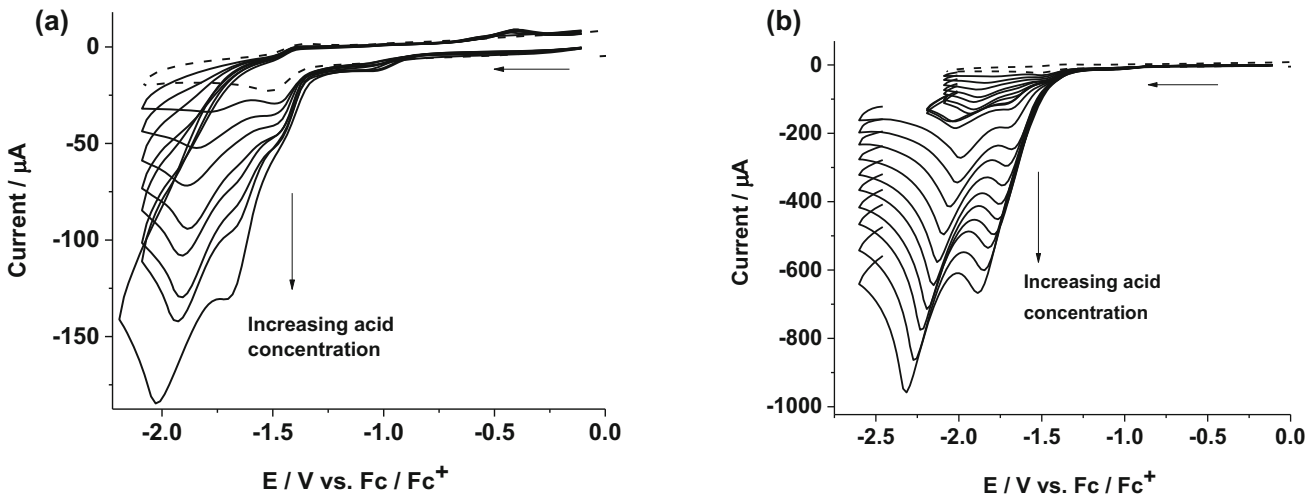

Figure 3. CVs for complex **1** (1 mM) in acetonitrile in the absence (—) and presence (—) of (a) 1–10 mM, and (b) 1–63 mM of TFA at a scan rate of 0.1 Vs^{-1}. The reverse scans have been omitted for clarity.

Complex **2** on the other hand, showed proton reduction activity with both AcOH and TFA. With AcOH (9 mM), a new peak appeared at −2.32 V the current for which increased upto 45 mM. On addition of 70 mM of acid, the solution turned colourless, suggesting that the complex was unstable at this concentration (Figure S10, SI). With TFA, two new peaks at −1.58 and −1.85 V were observed, on addition of 6 mM (6 equiv.) of acid (Figure 4), the currents levelled off after 50 mM of acid. The peaks at −1.68 (**1**) and −1.58 (**2**) V could be assigned to the complex participation in the electrocatalytic process and the peaks at −2.00 (**1**) and −1.85 (**2**) V to the homoconjugate adduct of TFA.[40a]

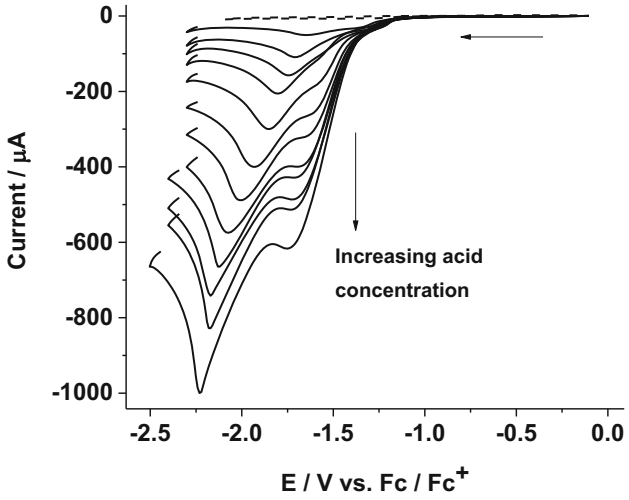

Figure 4. CVs for complex **2** (1 mM) in acetonitrile in the absence (—) and presence (—) of 1–38 mM of TFA at a scan rate of 0.1 Vs^{-1}. The reverse scans have been omitted for clarity.

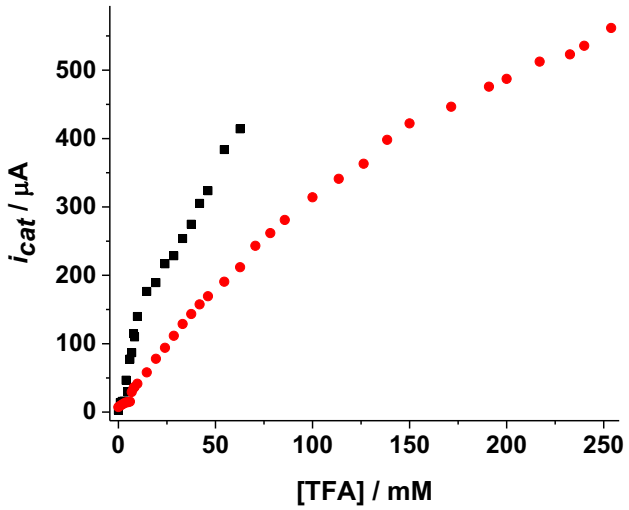

Figure 5. Plots of i_{cat} / µA *vs.* [TFA] / mM (peak 1) for complexes **1** (●) and **2** (■) in CH_3CN. Negative sign for i_{cat} has been ignored.

The increase in currents can be attributed to the electrocatalytic proton reduction activity (plots of i_{cat} *vs.* acid concentration) (Figure 5 and Figure S11, SI),[4b,40b] which was also confirmed by measuring the currents with acid, in the absence of catalyst (Figures S12–13, SI). The overpotential calculated by Evans method was 0.79 V (**1**), 0.67 V (**2**) with TFA and 0.82 V (**2**) with AcOH ($\eta = |E^{\circ}_{HA} - E_{cat}|$),[4b,40b] which was in the range for similar reported complexes (Table 2).[21–24]

Controlled potential electrolysis at a fixed potential (of peak 1) was carried out for complexes (0.25 mM) **1** and **2** in the presence of TFA (24 mM) to further support the electrocatalytic generation of H_2 (Figure S14, SI). Though some uncatalyzed proton reduction was detected for only acid, however, higher charge measured for the specified time period in the presence of **1** and **2** supported their catalytic activity (Figure S14, SI).[41]

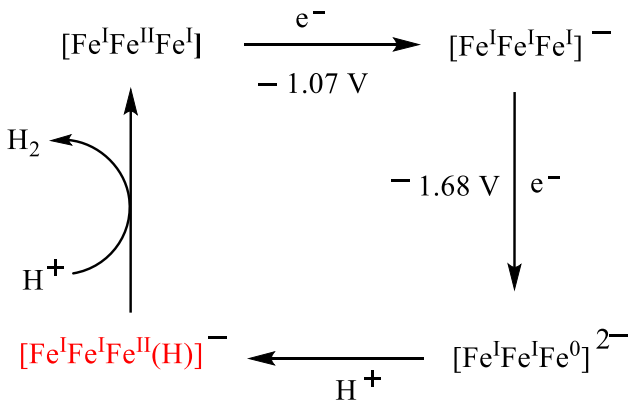

Scheme 2. Probable proton reduction mechanism for complex **1**.

Further, dependence of catalytic currents on the acid and substrate concentrations can be used to determine the order of the reaction for a catalytic process (Equation 1).[42] With constant [catalyst] but increasing [acid], a linear plot of i_{cat} vs. [acid] indicates a second-order reaction with respect to [H^+] (Figure 5) (Equation 1)[42] while for fixed [acid] but increasing [catalyst], a linear plot of i_{cat} vs. [catalyst] suggests a first-order reaction with respect to [catalyst] (Figures S15 and S16, SI). For CVs obtained with varying concentrations of complexes **1** and **2** in the presence of 19 mM TFA see Figures S15a and S16a, SI.[43a] Overall, the H_2 evolution reaction can be kinetically represented as rate = k_1[catalyst][acid]^2, where k_1 is the observed rate constant for the reaction. Furthermore, k_{obs} can be used to obtain the turnover frequency (*TOF*) of the catalyst under pseudo-first-order (Equation 2).[43]

$$\frac{i_{cat}}{i_p} = \frac{n}{0.446}\sqrt{\frac{RTk_{obs}}{Fv}} \quad (1)$$

$$\text{and} \qquad k_{obs} = k_1[H^+] \quad (2)$$

where i_p is the peak current in the absence of acid, i_{cat} is the peak current in the presence of an acid, R is the ideal gas constant, n is the number of electrons involved in the catalytic process, F is Faraday's constant, T is the temperature in Kelvin (298 K) and *v* is the scan rate.

$\frac{i_{cat}}{i_p}$ values of 23 and 40.3 corresponded to k_{obs} (s^{-1}) of ~ 102 (250 mM TFA) and ~ 315 (50 mM TFA) for complexes **1** and **2**, respectively (Figures S17 and S18, SI) (i_p calculated at −1.51 (**1**), −1.20 V (**2**); and i_{cat} at −1.68 (**1**), −1.58 V (**2**)).[43] The contribution of the reduction of TFA (i_{acid}) at the electrode was taken into account for calculating $\frac{i_{cat}}{i_p}$ and *TOF* values.[44] For calculating the *TOF* values CVs were measured with a systematic increase in the concentration of TFA until constant values of *TOF* were obtained.[44]

Complexes **1** and **2** showed faster catalysis (higher i_{cat}/i_p and *TOF*) but similar overpotential as the other analogous reported complexes (Table 2).

Two electrochemical (E) and two chemical (C) (protonation) processes are required for the electrocatalytic evolution of hydrogen. A tentative mechanism for proton reduction by complex **1** is shown in Scheme 2. Based on the CVs discussed earlier, an EECC (E = electrochemical; C = chemical) mechanism has been proposed. A similar mechanism has been proposed for the triiron clusters reported in the literature, which also supports the speculated catalytic steps.[21a,b,22–24] Complex **1** is reduced in two steps, followed by two subsequent protonation steps to produce hydrogen. On the other hand, an EECC or ECEC mechanism can be speculated for complex **2**. Further the proximity between the metal centres for complex **1** also indicates co-operativity effect between the metal centres (Fe(1)-Fe(2) = 2.6569(8); Fe(2)-Fe(3) = 2.5611(9) Å). Moreover, it is also plausible for the intermediate $[Fe^{I}Fe^{I}Fe^{II}(H)]^{-}$ to be first reduced and then protonated in the second step to generate hydrogen i.e. E(ECEC) mechanism. An EECC mechanism has also been proposed for photo-catalytic H_2 evolution in CH_3CN/H_2O (1:1, 2:1, 1:2) with complex **2** as the catalyst.[16b]

4. Conclusions

Reaction of triirondodecacarnonyl with 2-mercaptobenzimidazole was carried out to synthesize the diiron monothiolate-bridged complex $[Fe_2(CO)_6(\mu\text{-}2\text{-mercaptobenzimidazole})_2]$ **2** but instead a triiron carbene cluster $[Fe_3(C_7H_6N_2)(\mu_3\text{-}S)_2(CO)_8]$ **1** was obtained as a by-product (major). Electrochemical investigations of complexes **1** and **2** were performed in the presence of AcOH and TFA. Both the complexes were found to be efficient catalysts for the production of hydrogen. *TOF* values 102 (**1**) and 315 s^{-1} (**2**) hint towards their moderate performances as electrocatalysts in the presence of acid (TFA). The N-containing ligand in the organometallic clusters could play a pivotal role in electrocatalysis by providing extra binding sites at the N-atom or providing the right basicity to the system as a whole to affect its redox behaviour. However, further computational and bulk electrolysis studies are needed for identifying the intermediates involved and for predicting the proton reduction mechanism.

Supplementary Information (SI) The Supplementary information includes FTIR, UV-Vis, NMR, ESI-MS and electrochemical data. Supplementary Information is available at www.ias.ac.in/chemsci. CCDC 2002867 (for **1**) contains the supplementary crystallographic data for this article. These data can be obtained free of charge from the Cambridge Crystallographic Data Center via http://www.ccdc.cam.ac.uk/data_request/cif.

Acknowledgements

Financial support from the Council of Scientific & Industrial Research (CSIR), India (01(2957)/18/EMR-II) is gratefully acknowledged. SK-G is thankful to the University of Delhi for the instrumental facilities. NK is grateful to the University Grants Commission (UGC), New Delhi for the fellowship.

References

1. (a) Peters J W, Lanzilotta W N, Lemon B J and Seefeldt L C 1998 X-ray crystal structure of the Fe-only hydrogenase (CpI) from Clostridium pasteurianum to 1.8 Angstrom resolution *Science* **282** 1853; (b) Evans D J and Pickett C J 2003 Chemistry and the hydrogenases *Chem. Soc. Rev.* **32** 268; (c) Holm R H, Kennepohl P and Solomon E I 1999 Structural and functional aspects of metal sites in biology *Chem. Rev.* **96** 2239
2. a) De Lacey A L, Fernández V M, Rousset M and Cammack R, 2007 Activation and inactivation of hydrogenase function and the catalytic cycle: spectroelectrochemical studies *Chem. Rev.* **107** 4304; (b) Butt J N, Filipiak M and Hagen W R 1997 Direct electrochemistry of Megasphaera elsdenii iron hydrogenase *Eur. J. Biochem.* **245** 116; (c) Lubitz W, Ogata H, Rüdiger O and Reijerse E 2014 Hydrogenases *Chem. Rev.* **114** 4081
3. (a) Thoi V S, Sun Y, Long J R and Chang C J 2013 Complexes of earth-abundant metals for catalytic electrochemical hydrogen generation under aqueous conditions *Chem. Soc. Rev.* **42** 2388; (b) Ahmed M E and Dey A 2019 Recent developments in bioinspired modelling of [NiFe]- and [FeFe]-hydrogenases *Curr. Opin. Electrochem.* **15** 155; (c) Gao S, Liu Y, Shao Y, Jiang D and Duan Q 2020 Iron carbonyl compounds with aromatic dithiolate bridges as organometallic mimics of [FeFe] hydrogenases *Coord. Chem. Rev.* **402** 213081
4. (a) Queyriaux N, Jane R T, Massin J, Artero V and Chavarot-Kerlidou M 2015 Recent developments in

hydrogen evolving molecular cobalt(II)–polypyridyl catalysts *Coord. Chem. Rev.* **304** 3; (b) Felton G A N, Mebi C A, Petro B J, Vannucci A K, Evans D H, Glass R S and Lichtenberger D L 2009 Review of electrochemical studies of complexes containing the Fe2S2 core characteristic of [FeFe]-hydrogenases including catalysis by these complexes of the reduction of acids to form dihydrogen *J. Organomet. Chem.* **694** 2681; (c) Wang M, Chen L, Sun L, 2012 Recent progress in electrochemical hydrogen production with earth-abundant metal complexes as catalysts *Energy Environ. Sci.* **5** 6763

5. (a) Du P and Eisenberg R 2012 Catalysts made of earth-abundant elements (Co, Ni, Fe) for water splitting: recent progress and future challenges *Energy Environ. Sci.* **5** 6012; (b) Wittkamp F, Senger M, Stripp S T and Apfel U-P 2018 [FeFe]-Hydrogenases: recent developments and future perspectives *Chem. Commun.* **54** 5934; (c) Xu T, Chen D and Hu X 2015 Hydrogen-activating models of hydrogenases *Coord. Chem. Rev.* **303** 32; (d) Charreteur K, Kidder M, Capon J-F, Gloaguen F, Pétillon F Y, Schollhammer P and Talarmin J 2010 Effect of electron-withdrawing dithiolate bridge on the electron-transfer steps in diiron molecules related to [2Fe]H subsite of the [FeFe]-hydrogenases *Inorg. Chem.* **49** 2496
6. (a) Sun L, Åkermark B and Ott S 2005 Iron hydrogenase active site mimics in supramolecular systems aiming for light-driven hydrogen production *Coord. Chem. Rev.* **249** 1653; (b) Rauchfuss T B 2015 Diiron azadithiolates as models for the [FeFe]-hydrogenase active site and paradigm for the role of the second coordination sphere *Acc. Chem. Res.* **48** 2107; (c) Li Y and Rauchfuss T B 2016 Synthesis of diiron(I) dithiolato carbonyl complexes *Chem. Rev.* **116** 7043; (d) Darensbourg M Y, Lyon E J and Smee J J 2000 The bio-organometallic chemistry of active site iron in hydrogenases *Coord. Chem. Rev.* **206** 533; (e) Pandey I K, Natarajan M and Kaur-Ghumaan S 2015 Hydrogen generation: aromatic dithiolate-bridged metal carbonyl complexes as hydrogenase catalytic site models *J. Inorg. Biochem.* **143** 88; (f) Tschierlei S, Ott S and Lomoth R 2011 Spectroscopically characterized intermediates of catalytic H_2 formation by [FeFe] hydrogenase models *Energy Environ. Sci.* **4** 2340
7. (a) Lubitz W and Tumas W 2007 Hydrogen: an overview *Chem. Rev.* **107** 3900; (b) Tard C and Pickett C J 2009 Structural and functional analogues of the active sites of the [Fe]-, [NiFe]-, and [FeFe]-hydrogenases *Chem. Rev.* **109** 2245; (c) Song L C 2005 Investigations on butterfly Fe/S cluster S-centered anions $(\mu\text{-}S^{-})_2Fe_2(CO)_6$, $(\mu\text{-}S^{-})(\mu\text{-}RS)Fe_2(CO)_6$, and related species *Acc. Chem. Res.* **38** 21; (d) Zhang W, Lai W and R. Cao 2017 Energy-related small molecule activation reactions: oxygen reduction and hydrogen and oxygen evolution reactions catalyzed by porphyrin- and corrole-based systems *Chem. Rev.* **117** 3717; (e) Acar C, Dincer I and Zamfirescu C 2014 A review on selected heterogeneous photocatalysts for hydrogen production *Int. J. Energy Res.* **38** 1903
8. (a) Agarwal T and Kaur-Ghumaan S 2020 Mono- and dinuclear mimics of the [FeFe] hydrogenase enzyme featuring bis(monothiolato) and 1,3,5-triaza-7-phosphaadamantane ligands *Inorg. Chim. Acta* **504** 119442; (b) Day R J, Gross A J, Donovan E S, Fillo K D, Nichol G S and Felton G A N 2021 Spectroscopic and electrochemical comparison of [FeFe]-hydrogenase active-site inspired compounds: Diiron monobenzenethiolate compounds containing electron-donating and withdrawing groups *Polyhedron* **197** 115043; (c) Pandey I K, Natarajan M, Faujdar H, Hussain F, Stein M and Kaur-Ghumaan S 2018 Intramolecular stabilization of a catalytic [FeFe]-hydrogenase mimic investigated by experiment and theory *Dalton Trans.* **47** 4941; (d) Mebi C A, Karr D S and Noll B C 2013 Using naphthalene-2-thiolate ligands in the design of hydrogenase models with mild proton reduction overpotentials *Polyhedron* **50** 164; (e) Haley A L, Broadbent L N, McDaniel L S, Heckman S T, Hinkle C H, Gerasimchuk N N, Hershberger J C and Mebi C A 2016 [Fe–Fe] hydrogenase models: iron(I)-carbonyl clusters coupled to alpha- and para-toluenethiolate ligands *Polyhedron* **114** 218
9. Mebi C A, Karr D S and Gao R 2011 Diironhexacarbonyl clusters with imide and amine ligands: hydrogen evolution catalysts *J. Coord. Chem.* **64** 4397
10. (a) Liu X, Ibrahim S K, Tard C and Pickett C J 2005 Iron-only hydrogenase: synthetic, structural and reactivity studies of model compounds *Coord. Chem. Rev.* **249** 1641; (b) Ghosh A C, Duboc C and Gennari M 2021 Synergy between metals for small molecule activation: enzymes and bio-inspired complexes *Coord. Chem. Rev.* **428** 213606; (c) Gloaguen F and Rauchfuss T B 2009 Small molecule mimics of hydrogenases: hydrides and redox *Chem. Soc. Rev.* **38** 100
11. (a) Durgaprasad G, Bolligarla R and Das S K 2011 Synthesis, structural characterization and electrochemical studies of $[Fe_2(\mu\text{-}L)(CO)_6]$ and $[Fe_2(\mu\text{-}L)(CO)_5(PPh_3)]$ (L = pyrazine-2,3-dithiolate, quinoxaline-2,3-dithiolate and pyrido[2,3-b]pyrazine-2,3-dithiolate): Towards modeling the active site of [FeFe]–Hydrogenase *J. Organomet. Chem.* **696** 3097; (b) Schwartz L, Singh P S, Eriksson L, Lomoth R and Ott S 2008 Tuning the electronic properties of $Fe_2(\mu\text{-arenedithiolate})(CO)_6{-}n(PMe_3)n$ (n = 0, 2) complexes related to the [Fe–Fe]-hydrogenase active site *C. R. Chim.* **11** 875; (c) Durgaprasad G, Bolligarla R and Das S K 2012 Synthesis, crystal structure and electrocatalysis of 1,2-ene dithiolate bridged diiron carbonyl complexes in relevance to the active site of [FeFe]-hydrogenases *J. Organomet. Chem.* **706–707** 37; (d) Durgaprasad G and Das S K 2012 1,2-Ene dithiolate bridged diiron carbonyl-phosphine and -phosphite complexes in relevance to the active site of [FeFe]-hydrogenases: Synthesis, characterization and electrocatalysis *J. Organomet. Chem.* **717** 29; (e) Saxena D B, Khajuria R K and Suri O P 1982 Synthesis and spectral studies of 2-Mercaptobenzimidazole Derivatives *J. Heterocyclic Chem.* **19** 681
12. (a) Teramoto Y, Kubo K, Kume S and Mizuta T 2013 Formation of a hexacarbonyl diiron complex having a naphthalene-1,8-bis(phenylphosphido) bridge and the electrochemical behavior of its derivatives

Organometallics **32** 7014; (b) Petro B J, Vannucci A K, Lockett L T, Mebi C, Kottani R, Gruhn N E, Nichol G S, Goodyer P A J, Evans D H, Glass R S and Lichtenberger D L 2008 Photoelectron spectroscopy of dithiolatodiironhexacarbonyl models for the active site of [Fe–Fe] hydrogenases: insight into the reorganization energy of the "rotated" structure in the enzyme *J. Mol. Struct.* **890** 281

13. (a) Li P, Wang M, Pan J, Chen L, Wang N and Sun L 2008 [FeFe]-Hydrogenase active site models with relatively low reduction potentials: diiron dithiolate complexes containing rigid bridges *J. Inorg. Biochem.* **102** 952; (b) Samuel A P S, Co D T, Stern C L and Wasielewski M R 2010 Ultrafast photodriven intramolecular electron transfer from a zinc porphyrin to a readily reduced diiron hydrogenase model complex *J. Am. Chem. Soc*. **132** 8813
14. (a) Stanley J L, Heiden Z M, Rauchfuss T B, Wilson S R, De Gioia L and Zampella G 2008 Desymmetrized diiron azadithiolato carbonyls: a step toward modeling the iron-only hydrogenases *Organometallics* **27** 119; (b) Eilers G, Schwartz L, Stein M, Zampella G, De Gioia L, Ott S and Lomoth R 2007 Ligand versus metal protonation of an iron hydrogenase active site mimic *Chem. Eur. J.* **13** 7075; (c) Capon J F, Ezzaher S, Gloaguen F, Petillon F Y, Schollhammer P and Talarmin 2008 Electrochemical insights into the mechanisms of proton reduction by $[Fe_2(CO)_6\{\mu\text{-}SCH_2\text{-}N(R)CH_2S\}]$ complexes related to the [2Fe]H subsite of [FeFe]hydrogenase *J. Chem. Eur. J.* **14** 1954; (d) Schwartz L, Eriksson L, Lomoth R, Teixidor F, Vinas C and Ott S 2008 Influence of an electron-deficient bridging o-carborane on the electronic properties of an [FeFe] hydrogenase active site model *Dalton Trans.* 2379; (e) Capon J F, Gloaguen F, Schollhammer P and Talarmin J 2006 Activation of proton by the two-electron reduction of a di-iron organometallic complex *J. Electroanal. Chem.* **595** 47; (f) Felton G A N, Vannucci A K, Chen J, Lockett L T, Okumura N, Petro B J, Zakai U I, Evans D H, Glass R S and Lichtenberger D L 2007 Hydrogen generation from weak acids: electrochemical and computational studies of a diiron hydrogenase mimic *J. Am. Chem. Soc.* **129** 12521
15. (a) Donovan E S, McCormick J J, Nichol G S and Felton G A N 2012 Cyclic voltammetric studies of chlorine-substituted diiron benzenedithiolato hexacarbonyl electrocatalysts inspired by the [FeFe]-hydrogenase active site *Organometallics* **31** 8067; (b) Singh P S, Rudbeck H C, Huang P, Ezzaher S, Eriksson L, Stein M, Ott S and Lomoth R 2009 (I,0) Mixed-valence state of a diiron complex with pertinence to the [FeFe]-hydrogenase active site: An IR, EPR, and computational study *Inorg. Chem.* **48** 10883; (c) Yu Z, Wang M, Li P, Dong W, Wang F and Sun L 2008 Diiron dithiolate complexes containing intra-ligand NH···S hydrogen bonds: [FeFe] hydrogenase active site models for the electrochemical proton reduction of HOAc with low overpotential *Dalton Trans.* 2400
16. (a) Wen N, Xu F-F, Chen R-P and Du S-W 2014 Reversible carbonylation of [2Fe2S] model complexes with pendant quinoline or pyridine arms *J. Organomet. Chem.* **756** 61; (b) Zheng H-Q, Wang X-B, Hu J-Y, Zhao J-A, Du C-X, Fan Y-T and Hou H-W 2016 Photocatalytic H_2 evolution, structural effect and electron transfer mechanism based on four novel [2Fe2S] model complexes by photochemical splitting water *Solar Energy* **132** 373
17. Liu Q, Hu X, Liu S and An J 1992 Structural study on heterocyclic carbene-containing iron carbonyl cluster - structures of [cyclic] $Fe_3(CO)_8[CNHC(CH)_4CNH](\mu_3\text{-}S)_2$ *Chin. J. Struct. Chem.* **11** 104
18. Yang W, Fu Q, Zhao J, Cheng H-R and Shi Y-C 2014 Two $Fe_3(\mu_3\text{-}S)_2(CO)_8$ clusters with terminal N-heterocyclic carbenes *Acta Cryst.* **C70** 528
19. Liu X-F, Yu X-Y and Gao H-Q 2014 Reactions of cluster complex triiron enneacarbonyl disulfide with phosphine ligands *Mol. Cryst. Liq. Cryst.* **592** 229
20. (a) Zhuang B, Chen J, He L, Chen J, Zhou Z and Wu K 2004 Synthesis, structure and formation pathways of new Fe–S complexes containing $[Fe_2S_2]$-units in different valences, $[Fe_2S_2(CO)_4(PPh_3)_2]$, $[Fe_3S_2(CO)_6(PPh_3)_3]$ and $[Fe_4S_2(CO)_{10}]^{2-}$ and the origin of the $[Fe_2S_2]$-unit in metal–$[Fe_2S_2(CO)_6]$ complexes *J. Organomet. Chem.* **689** 2764; (b) Han J and Coucouvanis D 2005 Synthesis and structure of the organometallic $MFe_2(\mu_3\text{-}S)_2$ clusters (M = Mo or Fe) *Dalton Trans*. **7** 1234; (c) Windhager J, Rudolph M, Bräutigam S, Görls H and Weigand W 2007 Reactions of 1,2,4-trithiolane, 1,2,5-trithiepane, 1,2,5-trithiocane and 1,2,6-trithionane with nonacarbonyldiiron: structural determination and electrochemical investigation *Eur. J. Inorg. Chem*. **18** 2748
21. (a) Li Z, Zeng X, Niu Z and Liu X 2009 Electrocatalytic investigations of a tri-iron cluster towards hydrogen evolution and relevance to [FeFe]-hydrogenase *Electrochim. Acta* **54** 3638; (b) Mebi C A, Brigance K E and Bowman R B 2012 Biomimetic hydrogen generation catalyzed by triironnonacarbonyl disulfide cluster *J. Braz. Chem. Soc.* **23** 186
22. Gao W, Sun J, Li M, Åkermark T, Romare K, Sun L and Åkermark B 2011 Synthesis of a [3Fe2S] cluster with low redox potential from [2Fe2S] hydrogenase models: electrochemical and photochemical generation of hydrogen *Eur. J. Inorg. Chem.* **7** 1100
23. Kaiser M and Knör G 2015 Synthesis, characterization, and reactivity of functionalized trinuclear iron-sulfur clusters – a new class of bioinspired hydrogenase models *Eur. J. Inorg. Chem.* **25** 4199
24. Ghosh S and Hogarth G 2017 Trinuclear clusters containing 2-aminopyridinate/pyrimidinate ligands as electrocatalysts for proton reduction *J. Organomet. Chem.* **851** 57
25. (a) Agarwal T and Kaur-Ghumaan S 2019 HER catalysed by iron complexes without a Fe_2S_2 core: A review *Coord. Chem. Rev.* **397** 188; (b) Cheah M N, Tard C, Borg S J, Liu X, Ibrahim S K, Pickett C J and Best S P 2007 Modeling [Fe−Fe] hydrogenase: evidence for bridging carbonyl and distal iron coordination vacancy in an electrocatalytically competent proton reduction by an iron thiolate assembly that operates through Fe(0)−Fe(II) levels *J. Am. Chem. Soc.* **129** 11085; (c) Ghosh S, Hogarth G, Kabir S E, Miah A L, Salassa L, Sultana S and Garino C 2009 Synthesis and

molecular structure of $[Fe_4(CO)_{10}(\mu_4\text{-}O)(\kappa^2\text{-}dppn)]$ (dppn = 1,8-bis(diphenylphosphino)naphthalene): a missing piece in the $[M_4(CO)_{12}(\mu_4\text{-}E)]^{n-}$ (M = Fe, Ru; E = C, N, O; n = 2, 1, 0) puzzle, *Organometallics* **28** 7047; (d) Surawatanawong P and Hall M B 2010 Density functional study of the thermodynamics of hydrogen production by tetrairon hexathiolate, $Fe_4[\text{-}MeC(CH_2S)_3]_2(CO)_8$, a hydrogenase model *Inorg. Chem.* **49** 5737

26. (a) Bockman T M and Kochi J K 1987 Activation of triiron clusters by electron transfer. The pronounced modulation of ETC catalysis by bridging ligands *J. Am. Chem. Soc.* **109** 7725; (b) Femoni C, Iapalucci M C, Longoni G, Zacchini S and Zazzaroni E 2007 Synthesis and X-ray structure of the $[\{Fe_3(CO)_9(\mu_3\text{-}O)\}_2H]^{3-}$ trianion: dimerization of a metal carbonyl cluster via formation of an exceptionally short hydrogen bond *Dalton Trans*. **25** 2644; (c) Taheri A and Berben L A 2016 Tailoring electrocatalysts for selective CO_2 or H^+ reduction: iron carbonyl clusters as a case study *Inorg. Chem.* **55** 378
27. (a) Nguyen A D, Rail M D, Shanmugam M, Fettinger J C and Berben L A 2013 Electrocatalytic hydrogen evolution from water by a series of iron carbonyl clusters, *Inorg. Chem.* **52** 12847; (b) Ghosh S, Holt K B, Kabir S E, Richmond M G and Hogarth G 2015 Electrocatalytic proton reduction catalysed by the low-valent tetrairon-oxo cluster $[Fe_4(CO)_{10}(\kappa^2\text{-}dppn)(\mu_4\text{-}O)]^{2-}$ [dppn = 1,1′-bis(diphenylphosphino)naphthalene] *Dalton Trans.* **44** 5160; (c) Loewen N D, Thompson E J, Kagan M, Banales C L, Myers T W, Fettinger J C and Berben L A 2016 A pendant proton shuttle on $[Fe_4N(CO)_{12}]^-$ alters product selectivity in formate vs. H_2 production via the hydride $[H\text{–}Fe_4N(CO)_{12}]^-$ *Chem. Sci.* **7** 2728; (d) Wang X, Zhang T, Yang Q, Jiang S and Li B 2015 Synthesis and characterization of bio-inspired diiron complexes and their catalytic activity for direct hydroxylation of aromatic compounds *Eur. J. Inorg. Chem*. 817; (e) Rail M D and Berben L A 2011 Directing the reactivity of $[HFe_4N(CO)_{12}]^-$ toward H^+ or CO_2 reduction by understanding the electrocatalytic mechanism *J. Am. Chem. Soc.* **133** 18577
28. (a) Kleinhaus J T, Wittkamp F, Yadav S, Siegmund D and Apfel U-P 2021 [FeFe]-Hydrogenases: maturation and reactivity of enzymatic systems and overview of biomimetic models *Chem. Soc. Rev*. **50** 1668; (b) Zhang Y, Mei T, Yang D, Zhang Y, Wang B and Qu J 2017 Synthesis and reactivity of thiolate-bridged multi-iron complexes supported by cyclic (alkyl)(amino)carbene *Dalton Trans*. **46** 15888; (c) Wang Y, Zhang T, Li B, Jiang S, Sheng L 2015 Synthesis, characterization, electrochemical properties and catalytic reactivity of N-heterocyclic carbene-containing diiron complexes *RSC Adv*. **5** 29022
29. (a) Thomas C M, Liu T, Hall M B and Darensbourg M Y 2008 Series of mixed valent Fe(II)Fe(I) complexes that model the H_{ox} state of [FeFe]hydrogenase: redox properties, density-functional theory investigation, and reactivities with extrinsic CO *Inorg. Chem.* **47** 7009; (b) Song L-C, Luo X, Wang Y-Z, Gai B and Hu Q-M 2009 Synthesis, characterization and electrochemical behavior of some N-heterocyclic carbene-containing active site models of [FeFe]-hydrogenases *J. Organomet. Chem.* **694** 103; (c) Morvan D, Capon J-F, Gloaguen F, Pétillon F Y, Schollhammer P, Talarmin J, Yaouanc J-J, Michaud F and Kervarec N Modeling [FeFe] hydrogenase: synthesis and protonation of a diiron dithiolate complex containing a phosphine-N-heterocyclic-carbene ligand *J. Organomet. Chem.* **694** 2801; (d) Riener K, Haslinger S, Raba A, Högerl M P, Cokoja M, Herrmann W A and Kühn F E 2014 Chemistry of iron N-heterocyclic carbene complexes: syntheses, structures, reactivities, and catalytic applications *Chem. Rev*. **114** 5215; (e) Borthakur B and Phukan A K 2019 Can carbene decorated [FeFe]-hydrogenase model complexes catalytically produce dihydrogen? An insight from theory *Dalton Trans.* **48** 11298
30. (a) Sheldrick G M 2008 A short history of SHELX *Acta. Cryst*. **A64** 112; (b) Sheldrick G M 2015 Crystal structure refinement with SHELXL *Acta. Cryst*. **C71** 3; (c) Sheldrick G M 1997 SHELX-97: Program for crystal structure solution and refinement. University of Gottingen, Germany
31. (a) Farrugia L J 2012 WinGX and ORTEP for windows: an update *J. Appl. Cryst.* **45** 849; (b) Dolomanov O V, Bourhis L J, Gildea R J, Howard J A K and Puschmann H 2009 OLEX2: a complete structure solution, refinement and analysis program *J. Appl. Cryst*. **42** 339
32. (a) Hieber V W and Gruber J 1958 Zur Kenntnis der Eisencarbonylchalkogenide *Z. Anorg. Allg. Chem*. **296** 91; (b) Adams R D and Babin J E 1986 Ligand substitution vs. ligand addition. 1. Differences in reactivity between first- and third-row transition-metal clusters. Reactions of dimethylamine with the sulfidometal carbonyl clusters $M_3(CO)_9(\mu_3\text{-}S)_2$ (M = Fe, Os) *Inorg. Chem*. **25** 3418
33. Hong W-S, Wu C-Y, Lee C-S, Hwang W-S and Chiang M Y 2004 Novel iron carbonyl complexes from thiophene-2-carboxaldehyde thiosemicarbazone *J. Organomet. Chem.* **689** 277
34. Shi Y-C Cheng H-R and Cheng D-C 2013 A novel hexa-iron cluster with one disulfide and two Ph_2PCS^{3-} ligands *Acta Cryst*. **C69** 581
35. Yeo J, Cheah M H, Bondin M I and Best S P 2012 X-Ray spectroscopy and structure elucidation of reactive electrogenerated tri-iron carbonyl sulfide clusters *Aust. J. Chem.* **65** 241
36. (a) Rahaman A, Ghosh S, Unwin D G, Basak-Modi S, Holt K B, Kabir S E, Nordlander E, Richmond M G and Hogarth G 2014 Bioinspired hydrogenase models: the mixed-valence triiron complex $[Fe_3(CO)_7(\mu\text{-}edt)_2]$ and phosphine derivatives $[Fe_3(CO)_{7-x}(PPh_3)_x(\mu\text{-}edt)_2]$ (x = 1, 2) and $[Fe_3(CO)_5(\kappa^2\text{-}diphosphine)(\mu\text{-}edt)_2]$ as proton reduction catalysts *Organometallics* **33** 1356; (b) Liu S-T, Yan H, Hu X and Liu Q W 1992 Studies on cobalt clusters V. Syntheses and structures of sulfur-capped trinuclear cobalt carbonyl clusters containing bridged thiourea moiety *Acta Chim. Sinica* **50** 1173
37. Stromberg C J, Kohnhorst C L, Meter G A V, Rakowski E A, Caplins B C, Gutowski T A, et al. 2011 Terahertz, infrared and Raman vibrational assignments of [FeFe]-hydrogenase model compounds *Vibrat. Spectrosc.* **56** 219

38. (a) Kunkely H and Vogler A 1998 Photoreactivity of $Fe_2S_2(CO)_6$ originating from dσ* metal-to-ligand charge transfer excitation *J. Organomet. Chem.* **568** 291; (b) Tyler D R, Levenson R A and Gray H B 1978 Electronic structures and spectra of trinuclear carbonyl complexes *J. Am. Chem. Soc*. **100** 7888; (c) Farrugia L J, Evans C, Senn H M, Hänninen M M and Sillanpää R 2012 QTAIM View of metal–metal bonding in di- and trinuclear disulfido carbonyl clusters *Organometallics* **31** 2559
39. Elgrishi N, Rountree K J, McCarthy B D, Rountree E S, Eisenhart T T and Dempsey J L 2018 A practical beginner's guide to cyclic voltammetry *J. Chem. Educ.* **95** 197
40. (a) Fourmond V, Jacques P-A, Fontecave M and Artero V 2010 H_2 Evolution and molecular electrocatalysts: determination of overpotentials and effect of homoconjugation *Inorg. Chem*. **49** 10338; (b) Felton G A N, Glass R S, Lichtenberger D L and Evans D H 2006 Iron-only hydrogenase mimics. thermodynamic aspects of the use of electrochemistry to evaluate catalytic efficiency for hydrogen generation *Inorg. Chem*. **45** 9181
41. (a) Fu L-Z, Zhou L-L, Tang L-Z, Zhang Y-X and Zhan S-Z 2015 A molecular iron(III) electrocatalyst supported by amine-bis(phenolate) ligand for water reduction *Int. J. Hydrog. Energy* **40** 8688; (b) Costentin C, Drouet S, Robert M and Save´ant J-M 2012 Turnover numbers, turnover frequencies, and overpotential in molecular catalysis of electrochemical reactions. Cyclic voltammetry and preparative-scale electrolysis *J. Am. Chem. Soc*. **134** 11235; (c) Artero V and Save´ant J-M 2014 Toward the rational benchmarking of homogeneous H2-evolving catalysts *Energy Environ. Sci.* **7** 3808; (d) Hu C and Fan W Y 2019 Molybdenum carbonyl complexes as HER electrocatalysts *Mol. Catal*. **479** 110615
42. Carroll M E, Barton B E, Rauchfuss T B and Carroll P J 2012 Synthetic models for the active site of the [FeFe]-hydrogenase: catalytic proton reduction and the structure of the doubly protonated intermediate *J. Am. Chem. Soc.* **134** 18843
43. (a) Connor G P, Mayer K J, Tribble C S and McNamara W R 2014 Hydrogen evolution catalyzed by an iron polypyridyl complex in aqueous solutions *Inorg. Chem*. **53** 5408; (b) Yap C P, Hou K, Bengali A A and Fan W Y A Robust pentacoordinated iron(II) proton reduction catalyst stabilized by a tripodal phosphine *Inorg. Chem*. **56** 10926; (c) Rountree E S, McCarthy B D, Eisenhart T T and Dempsey J L 2014 Evaluation of homogeneous electrocatalysts by cyclic voltammetry *Inorg. Chem*. **53** 9983
44. Song L-C, Zhu L, Hu F-Q and Wang Y-X 2017 Studies on chemical reactivity and electrocatalysis of two acylmethyl(hydroxymethyl)pyridine Ligand-Containing [Fe]-hydrogenase models (2-$COCH_2$-6-$HOCH_2C_5H_3N$)$Fe(CO)_2L$ (L = η^1-SCOMe, η^1-2-SC_5H_4N) *Inorg. Chem.* **56** 15216